Computational Materials Science 111 (2016) 513–524

Contents lists available at ScienceDirect

Computational Materials Science

journal homepage: www.elsevier.com/locate/commatsci

Synergetic interplay between metal (Pt) and nonmetal (C) species in codoped TiO_2: A DFT+U study

Cecilia I.N. Morgade [a,b], Gabriela F. Cabeza [a,*]

[a] IFISUR-CONICET, Grupo de Materiales y Sistemas Catalíticos, Departamento de Física, Universidad Nacional del Sur, Av. Alem 1253, Bahía Blanca B8000CP, Argentina
[b] Universidad Tecnológica Nacional, 11 de Abril 461, Bahía Blanca B8000CP, Argentina

ARTICLE INFO

Article history:
Received 19 May 2015
Received in revised form 23 August 2015
Accepted 30 September 2015

Keywords:
TiO_2
Density functional theory
C–Pt-codoping
Electronic structure

ABSTRACT

The structural, energetic, magnetic and electronic properties of Pt–C-doped and Pt/C-codoped TiO_2 have been studied using first-principle calculations to elucidate the effect of the metal–nonmetal interactions.

Compared with other non-metals, C-doping induces the formation of complex structures on titania. From the analysis of the electronic structures of the C-doping system, band gap narrowing as well as the formation of localized gap states are observed in it. The calculated results are in agreement with the experimental absorptions observed in the UV–visible diffuse reflectance spectroscopy spectra. Based on our results, the main findings relating to Pt/C codoping are the formation of highly symmetric coordination-like compounds and the formation of impurity states in the band gap that could be propitious for the separation of photoexcited electron–hole pairs. Is especially remarkable the case of Pt/C@Ti-codoped TiO_2 which could be the most effective for the redox reaction of H_2O to produce H_2 and O_2 because it presents the greatest narrowing of the band gap, the lower shift of the conduction band and it is the only one that favorably modifies the position of valence band. All are necessary conditions for the reaction mentioned.

1. Introduction

The titania (TiO_2) has its own name not only for its technological but also for its catalytic applications, including WGS reaction [1] and photocatalysis among others, in its role as a photocatalyst in remedial reactions of environmental contaminants [2,3]. It has attracted interest in the study of possible modifications thereof, in order to optimize the absorption of solar radiation by changing its wide band gap (BG), its potential redox and the half-life of charge carriers generated in the titania activation.

In order to access the conduction band (CB), the electrons in the valence band (VB) need radiation of about 380 nm or less. In both polymorph systems, anatase (A) and rutile (R), the VB is located deep in energy generating holes with high oxidative power. However, the location of the CB bottom is close to reducing the potential of hydrogen [4], indicating weak reduction potentials. This effect is more pronounced in rutile than in anatase. On account of these differences in the position of the CB and indirect BG, anatase exhibits higher photoactivity [5].

Therefore, enhancing the oxide-reductive properties of titania (A and R) under energies corresponding to the visible solar spectrum, is a prerequisite for improving their activity and this implies a reduction in the value of their BG. Both, excited electrons from the valence band to the conduction band and holes generated in the process can migrate to the surface and react with electron donors or acceptors, respectively, or recombine releasing the absorbed energy. It is desirable that the titania modification generates not only a reduction in the required activation energy but also a decline in the recombination of the generated charges. Some studies have been published showing that the doping of the system with anionic species such as nitrogen, carbon and sulfur can potentially form new impurity levels closest to the valence band, reducing the width of the bandgap for maximum efficiency [6]. In particular, the C-doping has proved to be five times more effective than N-doping in the degradation of 4-chlorophenol with artificial light ($\lambda > 455$ nm) [7]. But nevertheless, despite recognition of the advantages of C-doping in the photocatalytic activity of titania, the understanding of electronic mechanisms involved in the process is still very limited.

Moreover, many studies of doped titania have been performed either in the anatase phase or in crystals which have different proportions of the most abundant polymorphs. Specifically, there is scant literature where the presence of C dopant in the rutile structure is examined, despite the well-known phase transformation from anatase to rutile at high temperatures. Certain technological

* Corresponding author. Tel.: +54 291 4595141; fax: +54 291 4595142.
E-mail address: gcabeza@uns.edu.ar (G.F. Cabeza).

http://dx.doi.org/10.1016/j.commatsci.2015.09.065
0927-0256/

processes are performed at temperatures belonging to the range of the transition temperature ranging between 823 K and 953 K [8]. Furthermore, Shen et al. found that the transformation from anatase to rutile occurs when heating a sample doped with C at temperatures near 623 K for a long time assuming that the C-doping could also modify the phase transition temperature of the system [9].

In relation to experimental studies, the preparation methods and precursors used as reagents in obtaining samples have shown significant influence on both polymorphs. The C impurities on doped systems were identified, using X-ray photoelectron spectroscopy (XPS), as carbides, carbonates and carboxyls depending on the preparation method [10]. The presence and concentration of vacancies, the distances between them and the doping atoms, the purity of the sample, the degree of crystallinity, grain size and temperature, pressure and working atmosphere, are parameters to be considered in the experimental work [6]. In particular, photo-reactivity is critically dependent on the defects in the material. The differences observed in experimental studies imply that the understanding of these types of structures in each case requires a rigorous theoretical study. The greatest difficulty in analyzing the results published in the literature arises from the different forms of theoretical representation used to model the system as well as the computational codes, dopant concentrations and the internal distances between atoms of impurities within the crystal [11].

With respect to the metal-doped, several studies show that noble metals such as Pt are usually deposited on TiO_2 as co-catalyst but some metal atoms diffuse into the bulk during sample preparation. However, there are few studies on Pt as a doping ion within the crystal. It has been shown that the Pt ion metal as dopant exhibits unique characteristics for the degradation of 4-chlorophenol and dicloacetate [12]. Furthermore, it has been experimentally observed that Pt impregnation in mesoporous nanocrystals of N-doped titania improves photocatalytic H_2 production considerably [13]. Moreover, recent studies on materials based on C-doped titania modified with Pt have shown an activity six times higher in the degradation of toluene in air compared to the activity observed in systems without the addition of Pt. The activity increment could be attributed to activation by visible light and the improvement in mobility processes and separation of charge carriers [14]. Other experimental results support that the mixed doping with transition metals and nonmetals greatly enhances the inhibition of recombination of charge carriers. Therefore, it is necessary to know accurately which ones are the contributions that each doping atom provides to the system. The accepted hypothesis is that the bands partially occupied close to the VB, resulting from the presence of nonmetal impurities, act as recombination centers (electrons of the partially occupied impurities states would annihilate the holes generated by the radiation absorbed) or as mobility reduction centers of charge carriers (the states of the metal impurities, near the CB, would immobilize the excited electrons) [15].

In this paper the structural, magnetic and electronic properties of C-doped titania in anatase and rutile structures are investigated considering different dopant sites, concentrations and carbon oxidation states. With the aim to obtain insight into the metal–nonmetal codoping effects, for example, by introducing additives of 5*d* and 2*p* elements we have performed a careful theoretical analysis of the energetic, structural and electronic properties of Pt/C-codoped anatase TiO_2. The innovation of this work is to provide a theoretical study of structural and electronic properties of TiO_2 systems codoped not studied thus far and as a potential trigger of new experimental studies to confirm our findings. The modification of properties in a controlled manner encourages the efficiency of the ab initio calculations.

2. Theoretical framework

Total energy DFT calculations were performed using the Vienna Ab-Initio Simulation Package (VASP) code [16] and the projector augmented-wave method (PAW) developed by Blöch to describe the ion–electron interactions [17]. We adopted the generalized gradient approximation for the exchange–correlation energy due to Perdew and Wang (GGA-PW91) [18]. The basis of plane waves were generated considering 4 valence electrons for Ti ($3d^3 4s^1$), 6 valence electrons for O ($2s^2p^4$), 10 electrons for Pt ($5d^9 6s^1$) and 4 electrons for C ($2s^2p^2$). The limit considered for the kinetic energy of expansion of plane waves was 450 eV. The Brillouin zone integration was performed on well-converged Monkhorst–Pack *k*-point meshes. For the *k*-point integration, we used $10 \times 10 \times 10$ mesh for the $(1 \times 1 \times 1)$ unit cells representation employed in systems with high concentrations of impurities (Fig. 1a), $3 \times 3 \times 3$ mesh for the $(3 \times 3 \times 1)$ anatase supercell of 108 atoms in order to represent the anatase doped system with low concentrations of impurities (Fig. 1b); $5 \times 5 \times 5$ mesh for C-doped rutile represented by a $(2 \times 2 \times 2)$ supercell (Fig. 1d) of 48 atoms [19]. The criterion for the self-consistent convergence of the total energy was 0.1 meV and the cell parameters were optimized using forces smaller than 20 meV/Å as conversion criteria. The value of Hubbard coefficient for corrections of Coulomb interactions of the Ti *d* electrons was optimized to a value of 8 eV. In this work, we use the Dudarev's approach [20] implemented in the Vienna Ab-Initio Simulation Package (VASP) through careful selection of U, achieving excellent matches with the experimental band gap and bulk modulus measured for the systems investigated. A research performed by our group, has just been published using the same value of U [21]. All calculations were performed at the spin polarized level.

For each optimized structure, both on rutile and anatase, the density of states (DOS) was calculated to obtain the corresponding electronic structure and band gap value (BG). The study was completed evaluating the corresponding magnetic moments per atom (μ in μ_B) and Bader charges [22] were calculated to conclude the analysis. The interatomic distances, angles and cell parameters were determined and the isosurfaces were obtained using VESTA [23].

3. Results and discussion

The main objective of this work is the analysis of the effect of Pt/C-codoping in titania. Moreover, in order to complete the analysis of carbon doping in TiO_2 we compare our theoretical results with published experimental ones in a special section.

Doping nature has extensive implications in the crystalline solid configuration and thus in their optical, structural and magnetic properties. The distortion of the symmetry with respect to the stoichiometric solid has not only structural, but also catalytic inferences accompanied by changes in electronic charge distribution and in its photocatalytic oxidation–reduction behavior. The degree of geometric distortion in the case of C addition in titania is largely dependent on the position of the impurity in the crystal structure which in turn determines the strongly anionic or cationic behavior thereof. The formation of CO_2 and CO_3 type structures within the crystal are specific to the unique nature of C characteristics compared to other nonmetals studied.

3.1. Carbon doping

In this section the results obtained for carbon impurities located in different sites and at different concentrations on both doped polymorphs, are discussed. The notation used is the following: first, the titania polymorphic type (A, R), then the type of site

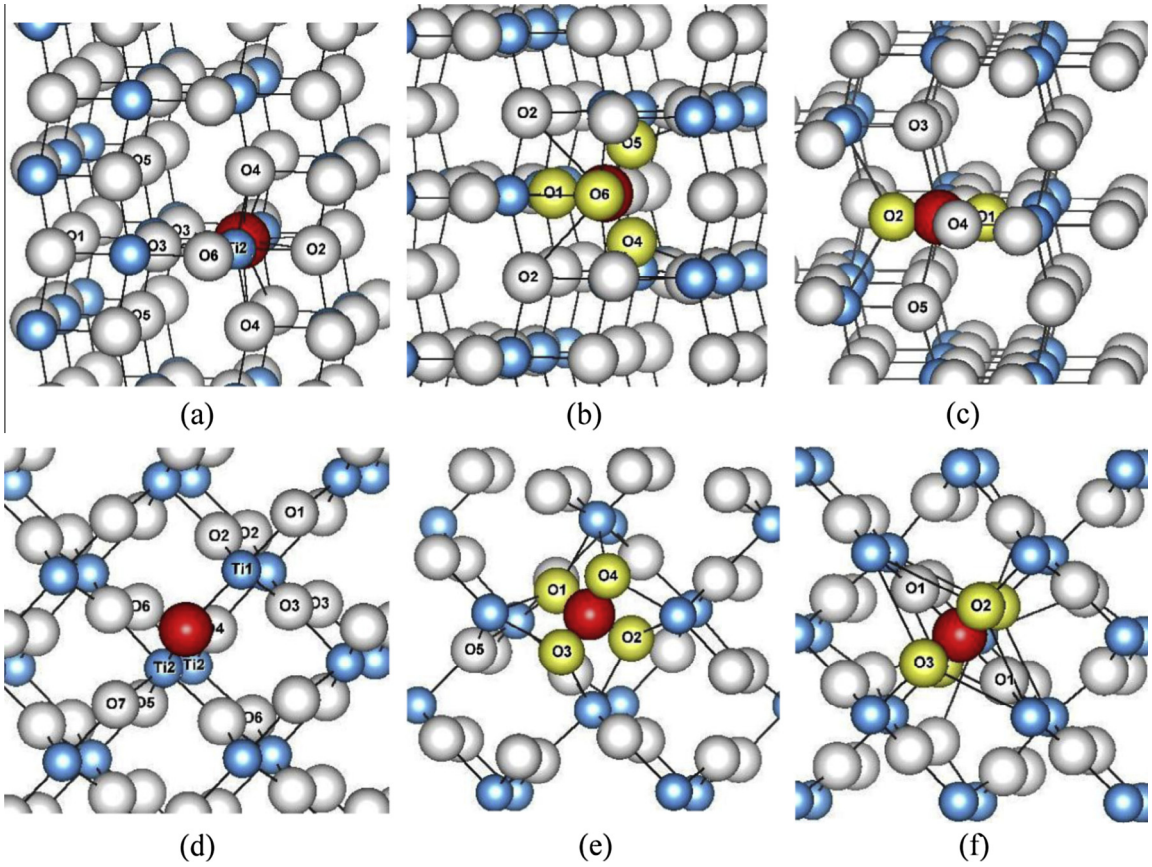

Fig. 1. Partial geometry of the models for C-doped anatase (top panel) and C-doped rutile (bottom panel) at low carbon concentrations; C@O (C in oxygen site) (a) and (d); Ci (C interstitial) (b) and (e) and C@Ti (C in titanium site) (c) and (f). The white spheres represent O atoms, the blue spheres represent the Ti atoms and the red sphere represent the C impurity. Information corresponding to numbered atoms is presented in Table 1. The oxygens involved in structures type carbonate are highlighted in yellow. (For interpretation of the references to color in this figure legend, the reader is referred to the web version of this article.)

accompanied by the weight percentage (wt%) of the carbon concentration (eg, ACi_3.66%). In the case of anatase, the study is completed with Pt codoping influence on the different oxidation states of carbon.

The formation energy is the energy needed to introduce the defect into the perfect crystal structure and, therefore, it is an important criterion to evaluate the relative difficulty for the incorporation of dopants into the anatase or rutile lattice. It is worth highlighting that we are interested in obtaining the relative stabilities of different dopant atoms; hence, the choice of E_C does not influence the conclusions.

The formation energies (E_{form}) or doping energy of three types of doped systems with different C-concentrations were calculated according to the following equations.

For the substitutional system (C@O, C@Ti):

$$E_{for} = E_{C\text{-doped}} - E_{pure} - n_C E_C + n_X E_X$$

For the interstitial system (C_i):

$$E_{for} = E_{C\text{-doped}} - E_{pure} - n_C E_C$$

where $E_{C\text{-doped}}$ and E_{pure} are the total energy of the supercells with and without substitutional (interstitial) C, respectively, n_C is the number of carbon atoms, E_C is the energy of an isolated C atom, n_X is the number of oxygen or titanium atoms substituted, E_X refers to the total energies of oxygen obtained from oxygen molecule energy (½ EO_2) or titanium obtained from isolated Ti energy. All energy values correspond to optimized systems.

3.1.1. Substitutional C-doping in oxygen site (C@O)

In order to represent the carbon-doped in an oxygen site, one oxygen atom was replaced by one carbon atom. This corresponds to a contribution in weight percent of 3.80 wt% (7.70 wt%) of carbon in anatase (rutile) for high concentrations and 0.42 wt% (0.94 wt%) for low concentrations, comparable to those used in some experimental studies. Low C-concentrations are computed in bigger supercells.

The cell parameters obtained for anatase are: $a = b = 3.956$ Å (exp. 3.782 Å) and $c = 9.761$ Å (exp. 9.502 Å). The system doped with high C-concentrations (AC@O_3.80%) has the following cell parameters: $a = 3.984$ Å, $b = 4.051$ Å and $c = 9.894$ Å; for low concentrations the values are: $a = 3.909$ Å, $b = 3.916$ Å and $c = 9.469$ Å (Fig. 1a). On average, apical bonds are lengthened by 3.16% and equatorial bonds by 1.67%.

Cell parameters obtained for undoped rutile are: $a = b = 4.733$ Å (exp. 4.586 Å) and $c = 3.100$ Å (exp. 2.954 Å). At high doping concentrations (RC@O_7.70%) the values are: $a = b = 4.878$ Å and $c = 3.123$ Å; when the percentage of C decreases, the obtained parameters are: $a = b = 4.860$ Å and $c = 3.147$ Å (Fig. 1d). In this case, the average increase in the value of the apical bonds is 2.42% and 1.86% for equatorial. In summary, the increase in the lattice parameters is more pronounced in the [001] direction of the doped anatase while the increment is developed in the directions [100] and [010] for rutile polymorph.

The formation energy values for the species in which one O atom is replaced by one C atom in the titania increase with decreasing concentration of C-dopant. For anatase, in order to obtain a concentration in weight of 3.80 wt% it has a cost of

0.46 eV whereas if the concentration in weight is 0.42 wt%, the cost rises to 3.18 eV. The same trend is obtained in the case of rutile whose values obtained are −0.07 eV and 1.10 eV to 7.70 wt% and 0.94 wt%, respectively.

For anatase, different doping concentrations do not affect the value of the magnetic moment per unit cell, being equal to 2 μ_B in both cases. For rutile, a polymorph 9% denser than anatase, whose concentrations studied are approximately twice those of anatase, the value of the magnetic moment increases when dopant concentration decreases, of 0.45–2.16 μ_B. The low concentration of impurities in rutile causes greater geometric distortion and increases local magnetization in the defect area (see Table 1).

The nature of the changes induced by the carbon in the electronic structure is controversial. The debate is between those who argue that a narrowing of BG [24,25] occurs and those who affirm that the modifications are a consequence of localized states formation in the band gap [26,27]. Our results indicate that doping provides the gap states that depend on the concentration of the defect (see Figs. 2 and A.1).

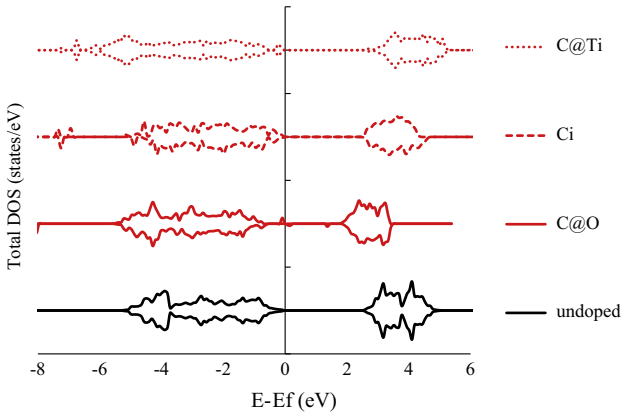

Fig. 2. Electronic density of states for C-doped rutile at low carbon concentration (see text). The lowest panel shows the bulk undoped rutile as reference.

Table 1
Principal distances between X_i (Ti—C) and Y_j (C—O) atoms nearby the dopant, charges and magnetic moment values (mm) for the same pairs of atoms, obtained for different types of C-doped (C@O–Ci–C@Ti) at high and low dopant concentration (wt%). The corresponding atoms numbered are showed in Fig. 1.

Anatase				Rutile			
Atoms X_i—Y_j	Dist. (Å) X_i—Y_j	Charges (e) X_i/Y_j	mm (μB) X_i/Y_j	Atoms X_i—Y_j	Dist. (Å) X_i—Y_j	Charges (e) X_i/Y_j	mm (μB) X_i/Y_j
C@O_3.80%				C@O_7.70%			
Ti1—C	2.174	2.64/−1.10	0.34/0.72	Ti1—C	2.146	2.63/−1.09	−/0.19
Ti1—O3	2.078	2.64/−1.36	0.34/–	Ti1—O1	2.063	2.63/−1.37	–
Ti1—O1	2.043	2.64/−1.35	0.34/–	Ti1—O2	2.050	2.63/−1.37	–
Ti1—O5	2.033	2.64/−1.37	0.34/–	Ti1—O3	2.050	2.63/−1.36	–
Ti2—O2	2.063	2.53/−1.36	–	Ti2—O5	2.017	2.56/−1.37	0.04/–
Ti2—O3	2.105	2.53/−1.36	–	Ti2—O6	2.044	2.56/−1.37	0.04/–
Ti2—C	2.064	2.53/−1.10	−/0.34	Ti2—C	2.219	2.56/−1.09	0.04/0.19
Ti2—O4	2.036	2.53/−1.36	–	Ti2—O7	2.017	2.56/−1.37	0.04/–
C@O_0.42%				C@O_0.94%			
Ti1—C	2.224	2.67/−1.16	0.34/0.72	Ti1—C	2.177	2.64/−1.08	−0.13/0.69
Ti1—O3	1.989	2.67/−1.38	0.34/–	Ti1—O1	2.080	2.64/−1.36	−0.13/–
Ti1—O1	2.012	2.67/−1.36	0.34/–	Ti1—O2	2.064	2.64/−1.36	−0.13/0.03
Ti1—O5	1.987	2.67/−1.38	0.34/–	Ti1—O3	2.064	2.64/−1.34	−0.13/0.03
Ti2—O2	2.025	2.67/−1.37	–	Ti2—O4	2.064	2.63/−1.38	0.30/–
Ti2—O3	2.027	2.67/−1.38	–	Ti2—O5	2.045	2.63/−1.34	0.30/–
Ti2—C	2.054	2.67/−1.16	−/0.72	Ti2—C	2.165	2.63/−1.08	0.30/0.69
Ti2—O4	1.994	2.67/−1.38	−/0.03	Ti2—O6	2.111	2.63/−1.35	0.30/–
Ti2—O6	1.960	2.67/−1.38	–	Ti2—O7	2.057	2.63/−1.37	0.30/–
Ci_3.66%				Ci_6.98%			
C—O1	1.250	1.59/−1.97	0.03/–	C—O1	2.874	1.92/−1.43	0.06/–
C—O2	3.175	1.59/−1.37	0.03/–	C—O2	1.327	1.92/−1.75	0.06/–
C—O3	2.062	1.59/−1.16	0.03/–	C—O3	1.287	1.92/−1.82	0.06/–
C—O4	2.214	1.59/−1.21	0.03/–	C—O4	2.591	1.92/−1.49	0.06/–
Ci_0.42%				Ci_0.93%			
C—O1	1.391	4.00/−1.83	–	C—O1	1.431	4.00/−1.81	–
C—O2	3.185	4.00/−1.43	−/−0.07	C—O2	1.431	4.00/−1.79	–
C—O3	2.753	4.00/−1.35	–	C—O3	1.428	4.00/−1.81	–
C—O4	1.426	4.00/−1.84	–	C—O4	1.428	4.00/−1.82	–
C—O5	1.426	4.00/−1.77	–	C—O5	3.616	4.00/−1.43	–
C—O6	1.452	4.00/−1.71	–				
C@Ti_4.23%				C@Ti_9.69%			
C—O1	1.298	4.00/−2.23	–	C—O1/2	2.128	4.00/−1.17	–
C—O2	1.298	4.00/−2.48	–	C—O3	1.226	4.00/−2.13	–
C—O3/4	2.032	4.00/−1.11	–	C—O4	1.226	4.00/−2.24	–
C@Ti_0.42%				C@Ti_0.97%			
C—O1	1.185	4.00/−2.04	–	C—O1	1.670	1.27/−1.18	–
C—O2	1.185	4.00/−2.05	–	C—O2/3	1.615	1.27/−1.07	–
C—O3/4	2.400	4.00/−1.27	–				
C—O5	2.400	4.00/−1.28	–				

m.m values less than 0.03 μ_B are indicated as –.

The electronic structures of the involved systems show that on both polymorphs, the CB moves to lower energy as a result of substitutional doping (C@O) and the width of the BG narrows (Figs. A.1 and A.2). The C-doping introduces band gap states of C 2*p* orbital character which are more localized and isolated at low concentrations of impurities. When the amount of C substituent is high, the bands in the BG are widened. For anatase, one up-spin gap state and one down-spin gap state are occupied while another down-spin state is unoccupied (see Table 2 and Fig. 3). The excitation energy from the filled up-spin state to the CB is 3.01 eV and from the filled down-spin to the CB is 2.92 eV. This explains the absorption in the range 400–600 nm observed in the UV–visible diffuse reflectance spectra (DRS) of C-doped TiO_2 samples [27]. In addition, the excitation energies from the filled up and down-spin gap states to the empty down-spin gap state are 2.21 eV and 2.13 eV which are smaller than the optical absorption energy of undoped anatase.

The effects of C-anion doping on rutile TiO_2 are similar to those previously described for anatase. The widths of the VB, CB and BG, as well as the peak positions in the BG measured from the CB bottom, are shown in Table 2. The BG narrowing is about 0.3 eV. Of the three states of C *2p* character (one up and two down) in the BG, the up-spin state is below the Fermi level and the down-spin states are unoccupied. The electron excitation is possible from the filled up-spin state to the CB (1.88 eV) or to the empty down-spin state (1.45 eV). The calculated results are in agreement with the experimentally "tail" observed in the UV–visible DRS spectra ($\lambda \sim$ 600–700 nm) [28]. At high C-concentration, the spin states of C 2*p* overlap with the VB.

When the carbon replaces an oxygen atom in anatase (rutile), it is reduced with a charge of $-1.16e$ ($-1.10e$). This negative charge is less than the charge that it would have the substituted oxygen ($-1.37e$). The oxygen atoms that are close to the impurity generally lose negative charge (from $-1.37e$ to $-1.35e$) and titanium atoms are reduced (Ti charge for undoped TiO_2 is 2.75*e*); this effect is more significant when the concentration of C-dopant is greater (see Table 1).

The elongation of the C—Ti distance with respect to O—Ti distance on both undoped structures (2.032 Å and 2.046 Å for anatase and rutile, respectively) is interpreted as a weakening of the bond because the electronegativity of C (2.55) is lower than that of O (3.44) and its greater atomic radius, 0.77 Å vs 0.66 Å, respectively.

The observed increase of the apical dipole moments of the octahedron for anatase (C@O_0.42%) has a double justification: on the one hand, modification of charges as a result of doping and on the other hand, the increased distances between ions (Table 3). This has been reported as a possible benefit of doping on the photocatalytic efficiency for a possible reduction in charge recombination [29].

3.1.2. Interstitial C-doped (C_i)

The high (low) concentrations in weight percent tested for interstitial C-doping are 3.66 wt% (0.42 wt%) in anatase (Fig. 1b) and 6.98 wt% (0.93 wt%) for rutile (Fig. 1e). In both polymorphs and for every concentration, a C atom at interstitial site was added (Ci) in the same cells and superlattices previously described.

Cell parameters obtained when titania is interstitially C-doped increase in all cases: $a = 4.03$ Å, $b = 4.07$ Å and $c = 9.88$ Å for ACi_3.66%; $a = 4.01$ Å, $b = 4.02$ Å and $c = 10.06$ Å for ACi_0.42%; $a = 5.03$ Å, $b = 4.95$ Å and $c = 3.08$ Å for RCi_6.98% and = 4.89 Å, $b = 4.90$ Å and $c = 3.17$ Å for RCi_0.93%. When rutile is doped with a high carbon concentration it suffers large deformation due to its high density; the angle values calculated are: $\alpha = 87.37°$, $\beta = 101.27°$ and $\gamma = 85.79°$ instead of 90° for undoped rutile.

Table 2
Widths of the valence band (VB), conduction band (CB) and band gap (BG). Location of states in the BG measured from the bottom of the BC (d: down – or: up) obtained for anatase and rutile for all doping cases studied.

	Anatase Undoped		Rutile Undoped	
BG (eV)	3.21		2.69	
VB (eV)	4.53		5.30	
CB (eV)	2.06		2.61	
BG states	–		–	
	C@O_3.80%	C@O_0.42%	C@O_7.70%	C@O 0.94%
BG (eV)	2.22	3.19	1.24	2.40
VB (eV)	5.32	4.61	6.63	5.05
CB (eV)	2.13	1.86	2.40	1.80
BG states	1.70 (d)	3.01 (u) – 2.92 (d) 0.80 (d)	0.91 (d)	1.88 (u) – 1.63 (d) 0.43 (d)
	Ci_3.66%	Ci_0.42%	Ci_6.98%	Ci_0.93%
BG (eV)	–	3.04	0.85	2.68
VB (eV)	7.62	4.36	7.76	5.37
CB (eV)	3.28	1.93	5.42	2.17
BG states	–	2.53 (u)	–	–
	C@Ti_4.23%	C@Ti_0.42%	C@Ti_9.69%	C@Ti_0.97%
BG (eV)	2.31	3.02	1.08	3.01
VB (eV)	5.22	4.27	6.70	6.11
CB (eV)	2.61	1.67	7.54	3.01
BG states	–	–	–	2.71 (u–d)

Table 3
Values of the dipole moments (apical and equatorial) calculated for C-anion doped anatase and rutile at the concentrations studied. Values are in Debyes.

Dipole moments (Db)	Anatase			Rutile		
	Undoped	C@O_3.80%	C@O_0.42%	Undoped	C@O_7.70%	C@O_0.94%
Apical	40.24	39.05	40.87	40.36	38.96	38.88
Equatorial	39.98	36.01	37.38	39.95	38.45	38.61

Unlike the case of C-anion doped titania the addition of one C atom in an interstitial position decreases the energy of formation. For anatase, the value is −2.07 eV (−6.13 eV) for high (low) carbon concentrations; whereas, for rutile, the corresponding value is −4.55 eV (−6.58 eV). These are all lower than those obtained for C@O cases.

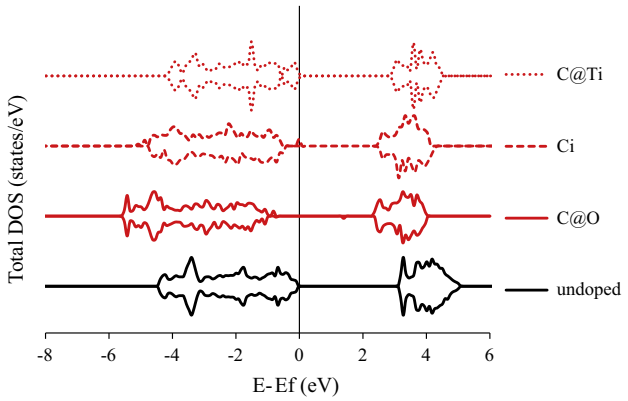

Fig. 3. Electronic density of states for C-doped anatase at low carbon concentration (see text). The lowest panel shows the bulk undoped anatase as reference.

Moreover, the magnetic moment per unit cell increases with decreasing carbon concentration; this augmentation is more important in the case of rutile. The calculated magnetic moments per cell are 1.74 μ_B (4.00 μ_B) for anatase at high (low) concentrations in weight and 1.11 μ_B (4.00 μ_B) in the case of rutile polymorph.

Our results show that interstitial carbon induces more complex features than when C substitutes an O atom of the lattice. In anatase, unlike the case of rutile, and for both C-doping concentrations studied, a displacement of the VB and CB toward lower energy values in comparison with the undoped system is observed (Figs. 4 and 5). At high concentrations of the C_i the C 1*s* band appears, at considerably lower energies (−25 eV), that are not observed in the undoped systems (not shown in figure). This observation is consistent with the binding energy shift observed in XPS spectra [30] in both regions C 1*s* and O 1*s*, indicating that carbons can be indeed incorporated into the lattice at lower calcination temperatures even in the absence of external carbon precursors. At low carbon concentrations, only one up-spin state is observed at 2.53 eV from the CB bottom, crossed by the Fermi level. The excess

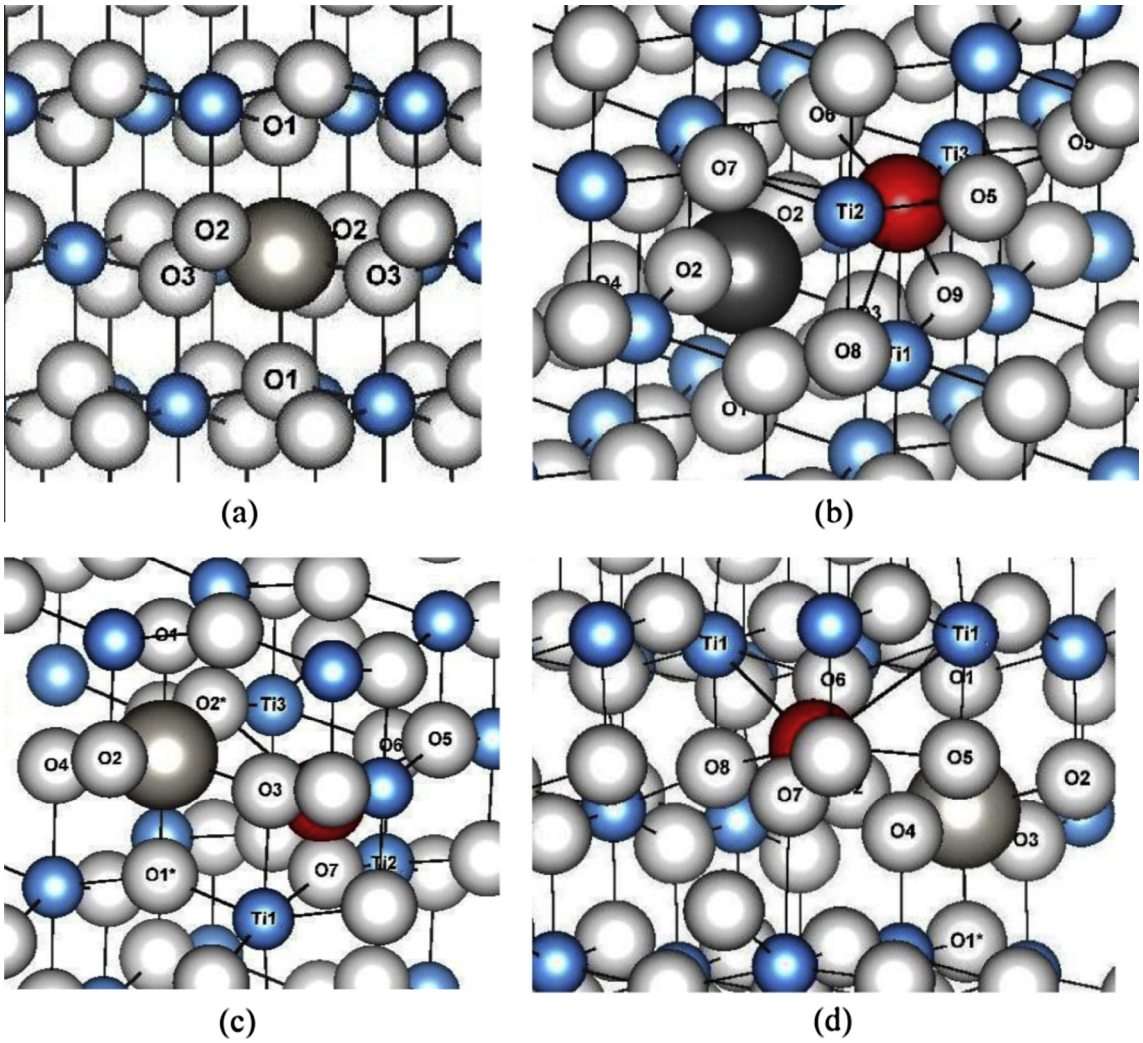

Fig. 4. Partial geometry of the models for Pt-doped anatase (a) and Pt/C-codoped anatase for one substitutional C atom in O site (b), one interstitial C atom nearby a Pt atom (c) and one substitutional C atom in Ti site (d). The white spheres represent O atoms, the blue spheres represent the Ti atoms, the gray sphere represents the Pt atom and the red sphere represents the C impurity. Information corresponding to numbered atoms is listed in Table 4. (For interpretation of the references to color in this figure legend, the reader is referred to the web version of this article.)

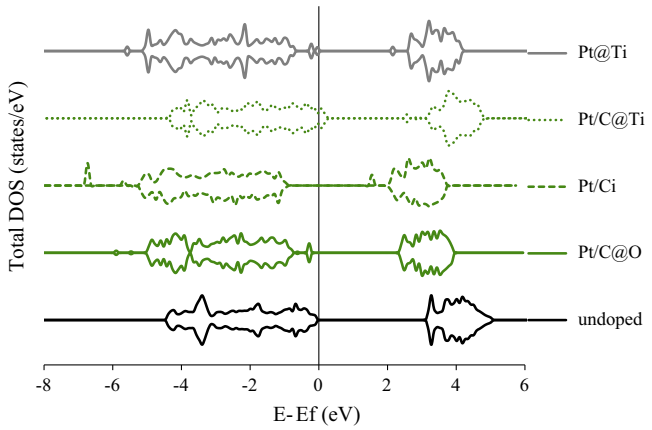

Fig. 5. Electronic density of states for Pt/C-codoped anatase TiO_2 at low carbon concentration (see text). The lowest panel shows the bulk undoped anatase as reference.

electrons introduced by the Ci impurity are transferred to Ti 3*d* states at the bottom of the CB and not to the C—O antibonding that lie within the titania conduction band. In any of the concentrations studied, the electronic structure of interstitially C-doped rutile does not present states in the BG. On both polymorphs, at high concentrations, a significant widening of both bands is observed due to overlapping bands; delocalized and continuous states are between the VB and CB providing a conductor behavior type (see Table 2).

In all cases of interstitial C-doping evaluated, the Ti atoms are reduced with respect to those of the undoped titania. This decrease in the positive charge of Ti is more pronounced in rutile at high C-concentrations (acquired 0.42*e*). The oxygen atom near the C acquires negative charge: 0.60*e* and 0.46*e* for high and low concentrations in anatase (O1) and 0.45*e* for both concentrations in rutile (O3) (Table 1). On the other hand, the carbon atom becomes positively charged in all cases: +1.59*e* (ACi_3.66%), +4.00*e* (ACi_0.42%), +1.91*e* (RCi_6.98%) and +4.00*e* (RCi_0.93%).

The formal oxidation state of carbon dopant ranges from −4 (as carbides with Ti—C bond) to +4 (as carbonate with C—O bond). In our case, the charge of +4*e* that acquires the carbon atom when it is at low concentrations is related to a tetrahedron-like structure (CO_4) with O—C—O angles of around 108° in the case of anatase and 105° for rutile. However, it is noteworthy to mention the formation of an angle of 119.1° for anatase, and two angles of 118.5° for rutile, both of about 120°, as well as those present in a carbonate-type structure, observed by some research groups [30,31]. In both polymorphs, the C—O distances are slightly lower than those of a single bond C—O (1.39/1.43 Å vs 1.54 Å). In relation to the atomic charges, it is noted (see Table 1) that the C is bonded to greatly reduced oxygen atoms (on average −1.80*e*). Similar observations were exposed by Gao et al. [32] who predict the formation of carbonate structures when studying the effect of a carbon +4*e* located on a Ti site. They set the value of the C charge using a $(2 \times 1 \times 1)$ supercell to represent the system and allowed both the cell and ions to relax. They found an increase in volume compatible with our interstitial doping case. One possible explanation for this could be that when a C replaces a Ti and it is allowed to relax with extensive freedom, the dopant finally moves toward an interstice in the lattice causing a major distortion. According to our calculations of formation energies, interstitial doping is less expensive than the substitution of a Ti atom by a C one. Furthermore, the density of states presented in Ref. [32] for anatase doped (C@Ti) is similar to those found by us for ACi_3.66%. In that case, they predicted a phase transition from semiconductor to conductor type Mott transition.

Experimental infrared spectroscopy studies (IR) of C-doped samples [27] showed several peaks between 2800 and 3000 cm^{-1} assigned to residual organic compounds; the bands around 2350 cm^{-1} correspond to gaseous CO_2 and the absorption peak at 1719 cm^{-1} was attributed to the formation of carbonate and the low-intensity bands at 1738, 1096 and 798 cm^{-1} are also indicative of carbonate ion, in consistence with our findings. In addition, recent experimental results on paramagnetic properties of carbon-doped TiO_2 [33] containing 0.42 wt% carbon showed an asymmetric shape of the signal of the EPR (electron paramagnetic resonance spectroscopy) that can be assigned to CO_2^- radicals. The authors assumed that CO_2^- radicals are located in the interstitial sites of TiO_2 lattice.

3.1.3. Substitutional C-doping in titanium site (C@Ti)

In order to complete the analysis of every C-doped titania system, we found it interesting to study the C-doping in a Ti site. The high (low) concentrations in weight studied, for substitutional C-doping in Ti-site (C@Ti) are 4.23 wt% (0.42 wt%) in the case of anatase and 9.69 wt% (0.97 wt%) for rutile. The cell parameters obtained are: $a = b = 4.05$ Å and $c = 9.09$ Å for AC@Ti_4.23%; $a = b = 4.07$ Å and $c = 10.06$ Å for AC@Ti_0.42%; $a = b = 4.73$ Å and $c = 3.21$ Å for RC@Ti_9.69% and $a = b = 4.53$ Å and $c = 3.05$ Å for RC@Ti_0.97%. Except for AC@Ti_0.42% sample, cell volumes decrease reaching a 19.92% for rutile with high C-concentration RC@Ti_ 9.69%.

The formation energies for C-cation doped systems are: 2.61 eV (AC@Ti_4.23%), 4.43 eV (AC@Ti_0.42%), 2.62 eV (RC@Ti_9.69%) and 6.89 eV (RC@Ti_0.97%). In all cases, C@Ti is energetically more expensive than Ci and C@O.

The evaluated C@Ti systems are non-magnetic. This situation is very different when the substituent of Ti is vanadium although the oxidation state of both doping elements is +4 [34].

For all systems studied, titanium atoms located far away from the impurity are reduced, acquiring approximately 0.04*e*, except for rutile at low C-concentration where all titanium atoms are oxidized losing about 0.04*e*.

When the doping concentration is high, the higher oxidation is suffered by the oxygens bonded equatorially to C (0.23*e* on average). In contrast, for a low concentration doped anatase, the oxygens which are far away from the impurity are those which suffer the greatest loss oxidation, being only 0.02*e*.

Moreover, in rutile doped with high carbon concentrations, greater oxidation is exhibited by the oxygen atoms away from C (0.31*e*). Regarding the apical oxygens bonded to C for anatase in both concentrations and rutile at high concentrations, they show the greatest reductions, with an average gain of 0.78*e*. However, for rutile doped at low C-concentrations, this reduction is only 0.05*e*.

The charge acquired by carbon atom in all cases, except in rutile at low C-concentrations, is +4*e* (see Table 1). These differences are strongly related to the C—O distances. In cases where the C acquires charge +4*e*, a structure type CO_2 is evidenced between C-dopant and oxygen atoms apically linked (O1 and O2). Bond lengths correspond to an intermediate distance between a covalent single bond C—O and a double one (see Table 1) and the O—C—O bond angle is 180°. Experimental studies using IR spectroscopy have reported absorption peaks near 2350 cm^{-1} compatible with structures type CO_2 [27]. While some works reported the finding of structures type CO_3 [34] or CO_4 [36] for this kind of dopant, our results are consistent with those published by the group of Yang [31] and they are even related to the experimental XPS band at 288.6 eV, which is attributed to the C=O bonds [34]. Remarkably, the RC@Ti_0.97% system showed the most marked differences

from others. It is the most unstable system, carbon charging is not +4*e* (+1.27*e*) which has also been observed by Di Valentin et al. [35] and oxygen atoms apically bonded thereto are much less reduced than in the other systems (see Table 1). It is important to highlight that there is no evidence of CO_2 formation as inner structures in the RC@Ti_0.97% system, which are indeed found in the rest of the systems studied when C is replacing Ti. In contrast, CO_4 structures are observed. Moreover, the C—O distances in the square planar CO_4 unit are greater than in the cases where the model structure observed is CO_2 (Fig. 1f) similar to what was reported by Yang [31].

Besides, it is the only system in which the band gap widens as a result of doping and that exhibits one state located at only 0.2 eV from VBM, in the BG. The excitation energy from the filled up/down-spin state to the CB is 2.71 eV (Table 2).

3.2. Pt doped (Pt@Ti) anatase

There have been made many studies of titanium oxides doped with certain transition metals such as Fe, Os, Y, La, Cr and V using different concentrations of the doping agent as well as synthetic routes in order to reduce the width of the band gap and the recombination of charge carriers when they are employed as co-dopants with nonmetals [37–39]. Choi et al. [40] indicate that Pt, V, Fe and Cr partially inhibit anatase–rutile transformation with temperature and increase the absorption of electromagnetic radiation extending to wavelengths corresponding to the visible spectrum. However, the studies with noble metals such as Ag, Au and Pt have been generally made with these metals deposited on the titania surfaces and not included in the crystal structure of the oxide. In this work, we present the study of Pt-doped anatase in Ti site as a preliminary step to the analysis of Pt-codoped with C anatase. The experimental work of Kim et al. [12] reinforces our motivation in the study of Pt as isolated dopant because they report significant improvements in the photo-activity of titania doped with Pt ion.

While we have also carried out studies for the Pt-doped titania with noble metals at low and high concentrations, this section only shows the results for low concentrations consistent with those values used for codoped-systems. The analyzed Pt concentration is 6.45 wt% and the models used to represent Pt-doped and Pt/C-codoped anatase are shown in Fig. 4.

The formation energy (E_{form}) or doping energy of the Pt-doped anatase (Pt@Ti) studied was calculated according to the following equation:

$$E_{for} = E_{Pt\text{-}doped} - E_{pure} - n_{Pt}E_{Pt} + n_{Ti}E_{Ti}$$

where $E_{Pt\text{-}doped}$ and E_{pure} are the total energy of the supercells with and without Pt, respectively, n_{Pt} is the number of platinum atoms, E_{Pt} is the energy of an isolated Pt atom, n_{Ti} is the number of titanium atoms substituted and E_{Ti} refers to the total energy of an isolated Ti atom. The calculated value for E_{for} is 2.34 eV.

The cell parameters obtained after optimization are reduced ($a = b = 3.94$ Å and $c = 9.69$ Å) with respect to undoped anatase, despite Pt being an element of the atomic radius greater than Ti. This relates particularly to the reduction of Pt—O equatorial bonds (see Table 4). The system preserves the tetrahedral structure of the system without impurities.

The Pt-doped system is non-magnetic as when C-doped titania in Ti site. DOS curves (Fig. 5) show that for the impurity concentration studied, the BG widens slightly as well as the VB in comparison with anatase undoped. On the contrary, the conduction band undergoes a reduction (see Table 5). There may also be a shift of both bands to lower energy values. The Pt-doping introduces three band gap states of Pt 5*d* and O 2*p* orbital character in the spin-up bands and also in the spin-down bands. Two of them, closest to the VBM, are occupied. The excitation energies from the filled states to the CB are 2.81 eV and 2.64 eV while de excitation energies from the filled states to the empty state are 2.37 eV and 2.20 eV.

In Pt-doped anatase, Ti atoms are oxidized losing, on average, 0.01*e*; the O atoms coordinated to Pt impurity are reduced (0.16*e*) and the Pt atom becomes positively charged (1.81*e*) similar to the charge that would have a Ti atom in the same site (2.74e).

Table 4
Principal distances between X_i (Pt—C) and Y_j (C—O) atoms nearby the dopant, charges and magnetic moment values (mm) for the same pairs of atoms, obtained for Pt-doped anatase and Pt/C codoped anatase (Pt/C@O–Pt/Ci–Pt/C@Ti) at low dopant concentration (wt%). The corresponding atoms numbered are showed in Fig. 2. The atoms marked with * are shown in Fig. 4.

Pt@Ti				Pt/C@O			
Atoms X_i—Y_j	Dist. (Å) X_i—Y_j	Charges (*e*) X_i/Y_j	mm (μB) X_i/Y_j	Atoms X_i—Y_j	Dist. (Å) X_i—Y_j	Charges (*e*) X_i/Y_j	mm (μB) X_i/Y_j
Pt—O1	2.037	2.74/−1.22	–	Pt—O1/2	2.055	1.76/−1.21	–
Pt—O2	2.017	2.74/−1.21	–	Pt—O3/4	2.051	1.76/−1.20	–
Pt—O3	2.017	2.74/−1.22	–	Pt—C	6.085	1.76/−1.09	–
Pt—O4	2.017	2.74/−1.20	–	C—O5	2.876	−1.09/−1.35	–
				C—O6/7	2.867	−1.09/−1.34	–
				C—O8	2.690	−1.09/−1.36	–
				C—Ti1/2	2.114	−1.09/2.66	–
				C—Ti3	2.242	−1.09/2.61	–
Pt/C_i				Pt/C@Ti			
Pt—O1/2*	2.047	1.76/−1.19	–	Pt—O1*	2.066	1.73/−1.21	–
Pt—O1*	2.070	1.76/−1.26	–	Pt—O1	2.049	1.73/−1.19	–
Pt—O3	2.091	1.76/−1.16	–	Pt—O2	2.062	1.73/−1.20	–
Pt—O4	2.044	1.76/−1.18	–	Pt—O3	2.088	1.73/−1.25	–
Pt—O2	2.049	1.76/−1.21	–	Pt—O4	1.994	1.73/−1.04	–
Pt—C	2.993	1.76/1.63	–	Pt—C	4.858	1.73/4.00	–
C—Ti1	2.750	1.63/2.22	−/1.05	C—O5	2.310	4.00/−1.27	–
C—Ti2	2.770	1.63/2.73	–	C—O6	1.201	4.00/−2.10	–
C—Ti3	2.976	1.63/2.35	−/1.02	C—O7	1.175	4.00/−2.05	–
C—O2*	2.501	1.63/−1.17	–	C—O8	2.310	4.00/−1.27	–
C—O5	2.499	1.63/−1.34	–	C—O9/10	3.111	4.00/−1.38	–
C—O6	2.313	1.63/−1.34	–	C—Ti1	2.927	4.00/2.75	–
C—O7	1.208	1.63/−1.93	–				

m.m values less than 0.03 μ_B are indicated as –.

Table 5
Widths of the valence band (VB), conduction band (CB) and band gap (BG). Location of states in the BG measured from the bottom of the BC (d: down – or: up) obtained for Pt-doped anatase and Pt/C codoped anatase.

	Pt@Ti	Pt/C@O	Pt/Ci	Pt/C@Ti
BG (eV)	3.34	3.20	3.04	3.03
VB (eV)	4.57	4.41	4.61	4.66
CB (eV)	1.76	1.64	1.78	1.73
BG states	2.81 (u–d) – 2.64 (u–d) 0.44 (u–d)	3.03 (u–d) – 2.68 (u–d) 0.43 (u–d)	0.52 (u)	0.65 (u–d) – 0.32 (u–d)

3.3. Pt/C-codoped anatase TiO_2

We start this section by considering the equations used to obtain the formation or doping energies (E_{form}) of the codoped systems. Similarly to the previous cases studied, the energies were calculated according to the following expressions:

For the substitutional Pt/C-codoped system (Pt/C@O, Pt/C@Ti):

$$E_{for} = E_{doped} - E_{pure} - n_C E_C - n_{Pt} E_{Pt} + n_X E_X$$

For the interstitial Pt/C-codoped system (Pt/C_i):

$$E_{for} = E_{doped} - E_{pure} - n_C E_C - n_{Pt} E_{Pt}$$

where E_{doped} and E_{pure} are the total energy of the supercells with and without dopants, respectively, n_{Pt} is the number of platinum atoms, E_{Pt} is the energy of an isolated Pt atom, n_C is the number of carbon atoms, E_C is the energy of an isolated C atom, n_X is the number of oxygen or titanium atoms substituted, E_X refers to the total energies of oxygen obtained from oxygen molecule energy (½ EO_2) or the energy of an isolated Ti atom. All energy values correspond to optimized systems.

3.3.1. Carbon in oxygen site (Pt/C@O)

Calculations to study Pt/C@O codoped anatase at high and low concentrations of dopants were made, but only the results for the lowest concentration are presented in this section. The system was evaluated using a concentration in weight of 6.46 wt% Pt for substitutional Pt doping in Ti-site and 0.40 wt% for C-doping in O-site. The values of the parameters of the unit cell increased in all three directions after doping, where $a = b = 4.00$ Å and $c = 9.95$ Å. The calculated value for E_{for} is 2.58 eV.

The system is non-magnetic. From the electronic structure analysis it is deduced that the BG remains almost unchanged compared to undoped anatase (Table 5). The doping provides five up/down-spin states as a result of the hybridization of Pt 5*d*, O 2*p* and Ti 3*d* orbitals. Four of them located at 3.03 eV and 2.68 eV from the CB bottom and at 0.43 eV and 0.87 eV below the VB bottom, are occupied; the other empty impurity state, barely perceptible, is located at 0.43 eV with respect to CB bottom (Fig. 5).

The most striking feature for this codoping is the formation of coordination compounds within the crystal between Ti atoms, the C atom and many O atoms. This structure is observed for both, high and low concentrations of codoping; it is formed in two almost orthogonal planes; one of them (plane *yz*) contains the central carbon, three titaniums coordinated to it (Ti1, Ti2 and Ti3), O9 and O10 (see Fig. 6); on the other hand, four oxygen atoms located radially to carbon lie in the plane *xy* perpendicular to the first forming, among them, angles ranging between 85° and 88°. The C—O bonds are elevated approximately 27° to the *xy* plane containing the corresponding oxygen atoms (inset Fig. 6).

Bader analysis showed that the Ti bonded to the carbon atom are reduced approximately 0.10*e*. Meanwhile, the oxygens closest to the platinum atom are more oxidized than the other oxygen atoms, losing, on average, 0.17*e* (Table 4). When Pt is present in the lattice, the carbon is more oxidized (−1.09*e*) than when it is compared with the case of simple C-anion-doped anatase (−1.16*e*). This electrostatic-like attraction exerted by the metal produces an increase in the separation between the plane containing the carbon and the plane above it. This is evidenced by the distance between the C and the O located just on top of C: 3.75 Å for Pt/C-doping vs 3.47 Å for C-doping. The C—O distances shorter than 3 Å are marked in gray in Fig. 8a and b. When this effect is observed with greater intensity, for example, in the cases of high doping concentration, could lead to eventual fracture planes.

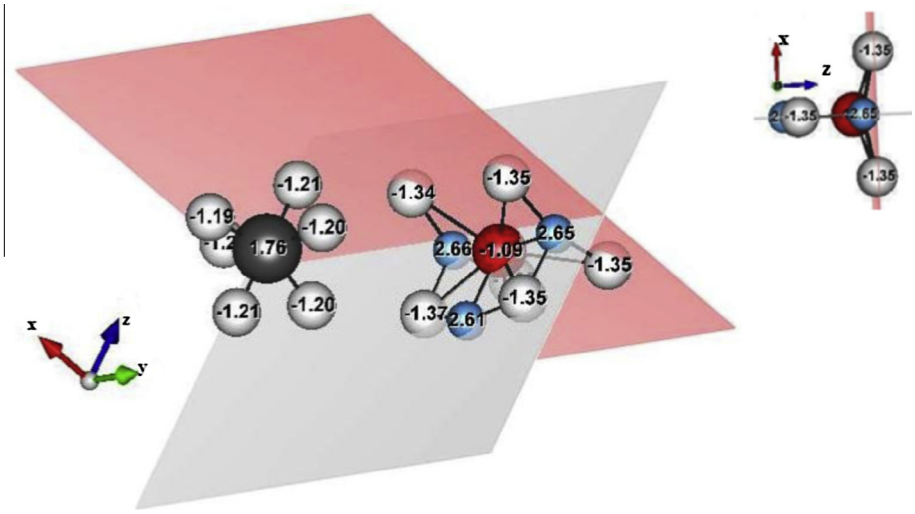

Fig. 6. Partial geometry of the model for the codoped Pt/C@O system. Formation of coordination compounds within the crystal between Ti atoms, the C atom and many O atoms. The corresponding Bader charges are indicated in the spheres. The planes are colored as a guide for the eye. For more details see text. (For interpretation of the references to colour in this figure legend, the reader is referred to the web version of this article.)

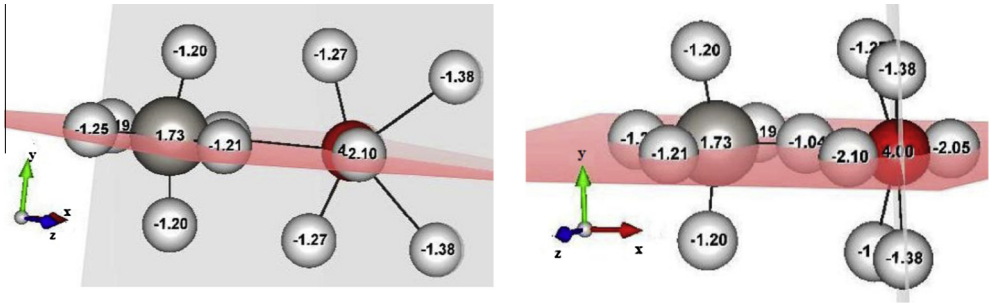

Fig. 7. Partial geometry of the model for the codoped Pt/C@Ti system. For more details see text.

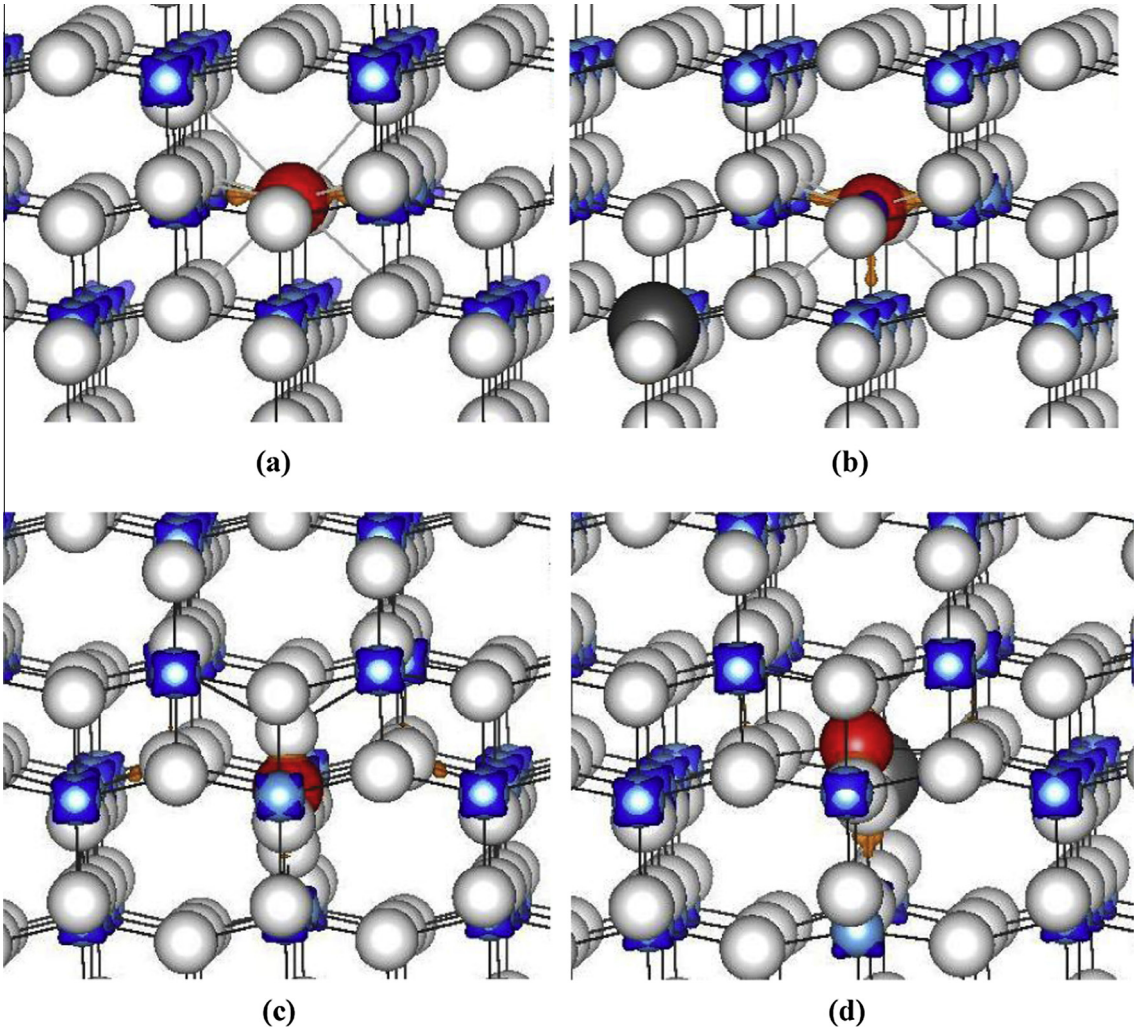

Fig. 8. Charge density differences of C-anion doping (a) and Pt/C-codoped (Pt/C@O) (b), C-cation doping (c) and Pt/C-codoped (Pt/C@Ti) (d) to visualize the effects of no-metal (C) and metal (Pt) in the anatase TiO_2 electronic structure. The orange and blue represent the positive and negative level ($e/Å^3$) isosurfaces, respectively, obtained using VESTA [22]. The corresponding level value is: $0.03e/Å^3$. The white spheres represent O atoms, the blue spheres represent the Ti atoms, the gray sphere represents the Pt atom and the red sphere represents the C impurity. (For interpretation of the references to color in this figure legend, the reader is referred to the web version of this article.)

3.3.2. Carbon interstitial (Pt/C_i)

For codoped Pt/Ci anatase, the optimized structure becomes more orthorhombic ($b > a$). Cell parameter values are greater than in the cases presented before: $a = 4.01$ Å, $b = 4.03$ Å and $c = 10.02$ Å. Angle values are: $\alpha = 90.17°$, $\beta = 89.99°$ and $\gamma = 89.98°$. Table 4 lists the optimized distances between atoms, the corresponding Bader charges and the magnetic moments. This system is magnetic with a magnetic moment of 2 μ_B. The calculated value for E_{for} is −1.33 eV.

The calculated DOS is shown in Fig. 5. From the electronic structure analysis it can be concluded that the BG narrows 0.17 eV compared to undoped anatase. The doping provides three up-spin states as a result of the hybridization of Pt 5*d*, Ti 3*d*, C 2*p* and O 2*p* orbitals. Two of them located at 0.52 eV and 1.36 eV below the VB bottom, are occupied; the other empty impurity up-spin gap state is located at 0.52 eV with respect to CB bottom.

Bader analysis showed that the O atoms closest to the platinum are oxidized and lose, on average, 0.18*e* (Table 4) and the platinum

charge is the same as in Pt/C@O. However, the C becomes positively charged without reaching the +4*e*, a charge that it has when is located in interstitial site without the presence of Pt metal. Finally, the Ti atoms bonded to the carbon atom are less reduced than in the case previously discussed.

3.3.3. Carbon in titanium site (Pt/C@Ti)

The anatase Pt/C@Ti codoped is also non-magnetic. Cell parameters increase as in the Pt/Ci case; the cell becomes orthorhombic: $a = 3.99$ Å, $b = 4.02$ Å and $c = 9.95$ Å representing an increase in volume of 4.48% compared with undoped anatase. The calculated value for E_{for} is 3.27 eV.

Among the different types of codoped analyzed in this work, Pt/C@Ti is the only case where the Fermi level crosses the valence band at about 0.2 eV VBM. The doping reduces the band gap of pure titania by shifting the position of valence band as evidenced by DOS curves (Fig. 5). According to what has been mentioned in the introduction, Pt/C@Ti-doped TiO_2 could be a good candidate for water splitting because it does not have a great effect on the CBM (0.02 eV) but increases the VBM edge significantly (0.28 eV). These two properties are essential because the CBM of TiO_2 is only slightly higher than the reducing potential of water, but the VBM of TiO_2 is far lower than the oxidizing potential of water. Additionally, the Pt–C codoping introduces two band gap up/down-spin states as a result of the hybridization of Pt 5*d*, O 2*p* and Ti 3*d* orbitals. Both, closest to the CBM, are unoccupied. Thus, the excitation energies from the VB to the empty states are 2.38 eV and 2.71 eV.

The Pt becomes positively charged and O atoms coordinated to it are oxidized, losing, on average, 0.19*e*. In turn, the C acquires a positive charge of +4*e*, as in the case of C-doped systems in Ti site. Two of the four O coordinated to C, are oxidized, losing 0.1*e* and the other two, more strongly bonded to C, are reduced, acquiring 0.7*e*. The C also coordinates with two Ti that lose approximately 0.18*e*. When carbon substitutes a titanium, it is "up" and the Ti—Ti bond increases from 3.95 Å (in Pt@Ti case) to 4.21 Å (Pt/C@Ti), and the original ∠Ti—Ti—Ti bond angle (179.4°) decreases to 147.45° (∠Ti—C—Ti), deforming the structure and acquiring a local internal geometry as in the case of Pt/C@O (Fig. 7).

In particular, two of the oxygen atoms (O6 and O7) coordinated to C forming a nearly flat bond (166.5°) with short C—O distance like CO_2. The other oxygen atoms lie in the plane *xy* perpendicular to the first forming, between them, angles of 138.67° (O5 and O8) and 80.66° (O9 and O10). With the aim to complete the visualization of the Pt/C-codoping effect on the local internal geometry observed, the corresponding differences in charge densities were performed (Fig. 8d).

A striking detail is that in the above-mentioned cases of codoping where these structures were observed, the metal–nonmetal distance is greater, showing a long-range interaction (6.09 Å for Pt/C@O, 4.86 Å for Pt/C@Ti and 3.01 Å for Pt/Ci). However, evidence of similarities found by us [41] and other authors in the study of N–V-codoping [42] suggest that this phenomenon is not due to carbon chemistry itself, but to the interaction metal–nonmetal.

4. Conclusions

Compared with other nonmetals, the C-doped induces the formation of complex structures on titania. Our results show that the carbon-doped reduces the width of the band gap, except in the case RC@Ti_0.97%. Remarkably, this system showed the most marked differences from others: it is the most unstable, carbon charging is not +4*e* and oxygen atoms apically bonded thereto suffer a much smaller reduction than in the other systems, and no evidence of CO_2 inner structures formation was found.

In all other systems studied, when titanium is replaced by a carbon, the oxidation state is +4 for carbon and −2 for oxygen, compatible with the observed CO_2-like structures.

The doping with interstitial carbon generates distorted tetrahedral structures in which carbonate-like species can be recognized. In these cases, the carbon oxidation state is +4.0 whereas is −1.8 for oxygen atoms.

The most significant characteristics observed in the codoped systems studied in this work are: firstly, the formation of highly symmetric coordination-like compounds, among C, Ti and O, where the central atom is C instead of a metal; secondly, the formation of impurity states in the BG that could be propitious for the separation of photoexcited electron–hole pairs. In the third place, the case of Pt/C@Ti-codoped TiO_2 is especially remarkable. It would be the most effective for the redox reaction of H_2O to produce H_2 and O_2 because it presents the greatest narrowing of the band gap (0.18 eV), the lower shift of the conduction band (0.02 eV) and it is the only one that favorably modifies the position of valence band (0.28 eV), which are all necessary conditions for the reaction mentioned.

Acknowledgements

This work was in part supported by the Consejo Nacional de Investigaciones Científicas y Técnicas (CONICET) (PIP: 02286) and by the Universidad Nacional del Sur (UNS) (PGI: 24/F055), Argentina. The authors thank Dra. C.I. Vignatti for their fruitful comments.

Appendix A. Supplementary material

Supplementary data associated with this article can be found, in the online version, at http://dx.doi.org/10.1016/j.commatsci.2015.09.065.

References

[1] C. Vignatti, M. Avila, C. Apesteguía, T. Garetto, Int. J. Hydrogen Energy 35 (2010) 7302.
[2] S. Banerjee, J. Gopal, P. Muralledharan, A. Tyagiand, B. Raj, Curr. Sci. 90 (2006) 1378.
[3] L. Jinwen, R. Han, Y. Zhao, H. Wang, W. Liu, T. Yu, Y. Zhang, J. Phys. Chem. C 115 (2011) 4507.
[4] Y. Gai, J. Li, S.-S. Li, J.-B. Xia, S.-H. Wei, Phys. Rev. Lett. 102 (2009) 036402.
[5] K. Palanivelu, J. Im, Y. Lee, Carbon Sci. 8 (2007) 214.
[6] J. Ananpattarachai, P. Kajitvichyanukul, S. Seraphin, J. Hazard. Mater. 168 (2009) 253.
[7] S. Sakthivel, H. Kisch, Angew. Chem., Int. Ed. 42 (2003) 4908.
[8] J. Zhang, M.J. Li, Z.C. Feng, J. Chen, C. Li, J. Phys. Chem. B 110 (2006) 927.
[9] M. Shen, Z. Wu, H. Huang, Y. Du, Z. Zou, P. Yang, Mater. Lett. 60 (2006) 693.
[10] E. Reyes-Garcia, Y. Sun, K. Reyes-Gil, D. Raftery, Solid State Nucl. Magn. Reson. 35 (2009) 74.
[11] E. Finazzi, C. Di Valentin, G. Pacchioni, A. Selloni, J. Chem. Phys. 129 (2008) 154113.
[12] S. Kim, S. Hwang, W. Choi, J. Phys. Chem. B 109 (2005) 24260.
[13] J. Ryu, S. Kim, Mater. Trans. 53 (2012) 2200.
[14] F. Dong, H. Wang, G. Sen, Z. Wu, S. Lee, J. Hazard. Mater. 187 (2011) 509.
[15] D. Zhang, M. Yang, Phys. Chem. Chem. Phys. 15 (2013) 18523.
[16] G. Kresse, J. Furthmuller, Phys. Rev. B 54 (1996) 11169.
[17] P. Blochl, Phys. Rev. B 50 (1994) 17953.
[18] J.P. Perdew, Y. Wang, Phys. Rev. B 33 (1986) 8822.
[19] M. Methfessel, A.T. Paxton, Phys. Rev. B 40 (1989) 3616.
[20] S. Dudarev, G. Botton, S. Savrasov, C. Humphreys, A. Sutton, Phys. Rev. B 57 (1998) 1505.
[21] C.I. Morgade, Ch. Vignatti, S. Avila, G.F. Cabeza, J. Mol. Catal. A: Chem. 407 (2015) 102–112.
[22] R.F.W. Bader, Atoms in Molecules: A Quantum Theory, Oxford University Press, Oxford, 1990.
[23] K. Momma, F. Izumi, J. Appl. Crystallogr. 44 (2011) 1272.
[24] S. Khan, M. Al-Shahry, W.B. Ingler Jr., Science 297 (2002) 2243.
[25] E. Barborini, A. Conti, I. Kholmanov, P. Miseri, C. Cepek, O. Sakho, R. Macovez, M. Sancrotti, Adv. Mater. 17 (2005) 1842.
[26] S. Sakthivel, H. Kisch, Angew. Chem., Int. Ed. 42 (2003) 4908.
[27] Y. Choi, T. Umebayashi, M. Yoshikawa, J. Mater. Sci. 39 (2004) 1837.

[28] K. Palanivelu, J.S. Im, Y.-S. Lee, Carbon Sci. 8 (2007) 214.
[29] Z. Zhao, Q. Liu, J. Phys. D: Appl. Phys. 41 (2008) 025105.
[30] Y. Park, W. Kim, H. Park, T. Tachikawa, T. Majima, W. Choi, Appl. Catal., B 91 (2009) 355.
[31] K. Yang, Y. Dai, B. Huang, M. Whangobo, J. Phys. Chem. C 113 (2009) 2624.
[32] H. Gao, C. Ding, D. Dai, J. of Mol. Struct. THEOCHEM 944 (2010) 156.
[33] A.A. Minnekhanov, D.M. Deygen, E.A. Konstantinova, A.S. Vorontsov, P.K. Kashkarov, Nanoscale Res. Lett. 7 (2012) 333.
[34] H. Kamisaka, T. Adachi, K. Yamashita, J. Chem. Phys. 123 (2005) 084704.
[35] C. Di Valentin, G. Pacchioni, A. Selloni, Chem. Mater. 17 (2005) 6656.
[36] W. Ren, Z. Ai, F. Jia, L. Zhang, X. Fan, Z. Zou, Appl. Cat., B 69 (2007) 138.
[37] H. Zhu, J. Liu, Comput. Mater. Sci. 85 (2014) 164.
[38] R. Jaiswala, N. Patel, D. Kotharia, A. Miotello, Appl. Cat., B 126 (2012) 47.
[39] V. Zainullina, V. Zhukov, V. Krasilnikov, M. Yanchenko, L. Buldakova, E. Polyakov, Phys. Solid State 52 (2010) 271.
[40] J. Choi, H. Park, M. Hoffmann, J. Phys. Chem. C 114 (2010) 783.
[41] The results obtained by us from the study of V/C and Pt/N-codoped anatase TiO_2 are in the process of writing to be sent to publish.
[42] Z. Zongyan, L. Zhaosheng, Z. Zhigang, Chem. Phys. Chem. 13 (2012) 3836.